

# Individual dynamics induces symmetry in network controllability

Chen Zhao,<sup>1</sup> Wen-Xu Wang,<sup>1</sup> Yang-Yu Liu,<sup>2,3,\*</sup> and Jean-Jacques Slotine<sup>4,5,†</sup>

<sup>1</sup>*School of Systems Science, Beijing Normal University, Beijing, 10085, P. R. China*

<sup>2</sup>*Channing Division of Network Medicine, Brigham and Women's Hospital,  
Harvard Medical School, Boston, Massachusetts 02115, USA*

<sup>3</sup>*Center for Complex Network Research and Department of Physics,  
Northeastern University, Boston, Massachusetts 02115, USA*

<sup>4</sup>*Nonlinear Systems Laboratory, Massachusetts Institute of Technology, Cambridge, Massachusetts, 02139, USA*

<sup>5</sup>*Department of Mechanical Engineering and Department of Brain and Cognitive Sciences,  
Massachusetts Institute of Technology, Cambridge, Massachusetts, 02139, USA*

Controlling complex networked systems to a desired state is a key research goal in contemporary science. Despite recent advances in studying the impact of network topology on controllability, a comprehensive understanding of the synergistic effect of network topology and individual dynamics on controllability is still lacking. Here we offer a theoretical study with particular interest in the diversity of dynamic units characterized by different types of individual dynamics. Interestingly, we find a global symmetry accounting for the invariance of controllability with respect to exchanging the densities of any two different types of dynamic units, irrespective of the network topology. The highest controllability arises at the global symmetry point, at which different types of dynamic units are of the same density. The lowest controllability occurs when all self-loops are either completely absent or present with identical weights. These findings further improve our understanding of network controllability and have implications for devising the optimal control of complex networked systems in a wide range of fields.

PACS numbers:

As a key notion in control theory, controllability denotes our ability to drive a dynamic system from any initial state to any desired final state in finite time [1, 2]. For the canonical linear time-invariant (LTI) system  $\dot{\mathbf{x}} = \mathbf{A}\mathbf{x} + \mathbf{B}\mathbf{u}$  with state vector  $\mathbf{x} \in \mathbb{R}^N$ , state matrix  $\mathbf{A} \in \mathbb{R}^{N \times N}$  and control matrix  $\mathbf{B} \in \mathbb{R}^{N \times M}$ , Kalman's rank condition  $\text{rank}[\mathbf{B}, \mathbf{A}\mathbf{B}, \dots, \mathbf{A}^{N-1}\mathbf{B}] = N$  is sufficient and necessary to assure controllability. Yet, in many cases system parameters are not exactly known, rendering classical controllability tests impossible. By assuming that system parameters are either fixed zeros or freely independent, structural control theory (SCT) helps us overcome this difficulty for linear time-invariant systems [3–7]. Quite recently, many research activities have been devoted to study the structural controllability of systems with complex network structure, where system parameters (e.g., the elements in  $\mathbf{A}$ , representing link weights or interaction strengths between nodes) are typically not precisely known, only the zero-nonzero pattern of  $\mathbf{A}$  is known [8–15]. Network controllability problem can be typically posed as a combinatorial optimization problem, i.e., identify a minimum set of driver nodes, with size denoted by  $N_D$ , whose control is sufficient to fully control the systems dynamics [8]. Other controllability related issues, e.g., energy cost, have also been extensively studied for complex networked systems [16–19]. While the intrinsic individual dynamics can be incorporated in the network model, it would be more natural and fruitful to consider their effect separately. Hence, most of the previous studies focused on the impact of network topology,

rather than the individual dynamics of nodes, on network controllability [8, 11].

If one explores the impact of individual dynamics on network controllability in the SCT framework, a specious result would be obtained — a single control input can make an arbitrarily large linear system controllable. Although this result as a special case of the minimum inputs theorem can be proved [8] and its implication was further emphasized in [20], this result is inconsistent with empirical situations, implying that the SCT is inapplicable in studying network controllability, if individual dynamics of nodes are imperative to be incorporated to capture the collective dynamic behavior of a networked system. To overcome this difficulty, and more importantly, to understand the impact of individual dynamics on network controllability, we revisit the key assumption of SCT, i.e., the independency of system parameters. We anticipate that major new insights can be obtained by relaxing this assumption, e.g., considering the natural diversity and similarity of individual dynamics. This also offers a more realistic characterization of many real-world networked systems where not all the system parameters are completely independent.

To solve the network controllability problem with dependent system parameters, we rely on the recently developed exact controllability theory (ECT) [21]. ECT enables us to systematically explore the role of individual dynamics in controlling complex systems with arbitrary network topology. In particular, we consider prototypical linear forms of individual dynamics (from first-order to high-orders) that

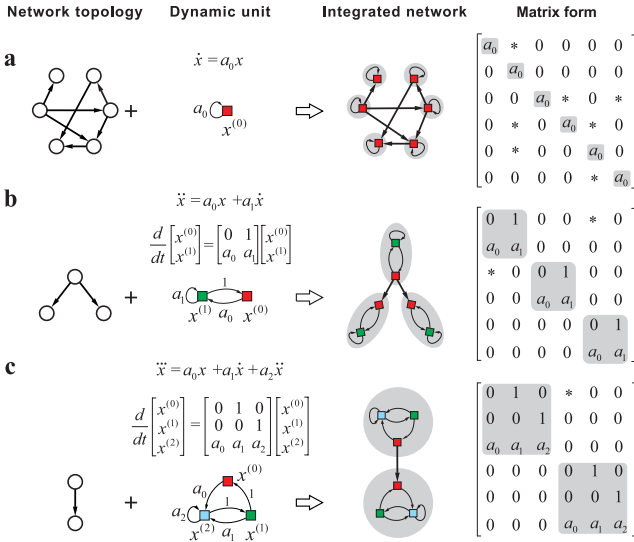


FIG. 1: Integration of network topology and (a) 1st-order, (b) 2nd-order and (c) 3rd-order intrinsic individual dynamics. For a  $d$ th-order individual dynamics  $x^{(d)} = a_0 x^{(0)} + a_1 x^{(1)} + \dots + a_{d-1} x^{(d-1)}$ , we denote each order by a colored square and the couplings among orders are characterized by links or self-loops. This graphical representation allows individual dynamics to be integrated with their coupling network topology, giving rise to a unified matrix that reflects the dynamics of the whole system. In particular, each dynamic unit in the unified matrix corresponds to a diagonal block and the nonzero elements (denoted by  $*$ ) apart from the blocks stand for the couplings among different dynamic units. Therefore, the original network consisting of  $N$  nodes with order  $d$  is represented in a  $dN \times dN$  matrix.

can be incorporated within the network representation of the whole system in a unified matrix form. This paradigm leads to the discovery of a striking symmetry in network controllability: if we exchange the fractions of any two types of dynamic units, the system's controllability (quantified by  $N_D$ ) remains the same. This exchange-invariant property gives rise to a global symmetry point, at which the highest controllability (i.e., lowest number of driver nodes) emerges. This symmetry-induced optimal controllability holds for any network topology and various categories of individual dynamics. We substantiate these findings numerically in a variety of network models.

Exact controllability theory (ECT) [21] claims that for arbitrary network topology and link weights characterized by the state matrix  $A$  in the LTI system  $\dot{\mathbf{x}} = A\mathbf{x} + B\mathbf{u}$ , the minimum number of driver nodes  $N_D$  required to be controlled by imposing independent signals to fully control the system is given by the maximum geometric multiplicity  $\max_i \{\mu(\lambda_i)\}$  of  $A$ 's eigenvalues  $\{\lambda_i\}$  [22–26]. Here  $\mu(\lambda_i) \equiv N - \text{rank}(\lambda_i I_N - A)$  is the geometric multiplicity of

the eigenvalue  $\lambda_i$  and  $I_N$  is the identity matrix. Calculating all the eigenvalues of  $A$  and subsequently counting their geometric multiplicities are generally applicable but computationally prohibitive for large networks. If  $A$  is symmetric, e.g., in undirected networks,  $N_D$  is simply given by the maximum algebraic multiplicity  $\max_i \{\delta(\lambda_i)\}$ , where  $\delta(\lambda_i)$  denotes the degeneracy of eigenvalue  $\lambda_i$ . Calculating  $N_D$  in the case of symmetric  $A$  is more computationally affordable than in the asymmetric case. Note that for structured systems where the elements in  $A$  are either fixed zeros or free independent parameters, ECT offers the same results as that of the SCT [21].

We first study the simplest case of first-order individual dynamics  $\dot{x}_i = a_0 x_i$ . The dynamical equations of a linear time-invariant control system associated with first-order individual dynamics [27] can be written as

$$\dot{\mathbf{x}} = \Lambda \mathbf{x} + A \mathbf{x} + B \mathbf{u} = \Phi \mathbf{x} + B \mathbf{u}, \quad (1)$$

where the vector  $\mathbf{x} = (x_1, \dots, x_N)^T$  captures the states of  $N$  nodes,  $\Lambda \in \mathbb{R}^{N \times N}$  is a diagonal matrix representing intrinsic individual dynamics of each node,  $A \in \mathbb{R}^{N \times N}$  denotes the coupling matrix or the weighted wiring diagram of the networked system, in which  $a_{ij}$  represents the weight of a directed link from node  $j$  to  $i$  (for undirected networks,  $a_{ij} = a_{ji}$ ).  $\mathbf{u} = (u_1, u_2, \dots, u_M)^T$  is the input vector of  $M$  independent signals,  $B \in \mathbb{R}^{N \times M}$  is the control matrix, and  $\Phi \equiv \Lambda + A$  is the state matrix. Without loss of generality, we assume  $\Lambda$  is a “constant” matrix over the field  $\mathbb{Q}$  (rational numbers), and  $A$  is a structured matrix over the field  $\mathbb{R}$  (real numbers). In other words, we assume all the entries in  $\Phi$  have been rescaled by the individual dynamics parameters. The resulting state matrix  $\Phi$  is usually called a *mixed matrix* with respect to  $(\mathbb{Q}, \mathbb{R})$  [28]. The first-order individual dynamics in  $\Phi$  is captured by self-loops in the network representation of  $\Phi$  (see Fig. 1a).  $N_D$  can then be determined by calculating the maximum geometric multiplicity  $\max_i \{\mu(\lambda_i)\}$  of  $\Phi$ 's eigenvalues.

We study two canonical network models (Erdős-Rényi and Scale-free) with random edge weights and a  $\rho_s$  fraction of nodes associated with identical individual dynamics (i.e., self-loops of identical weights). As shown in Fig. 2a,b, the fraction of driver nodes  $n_D \equiv N_D/N$  is symmetric about  $\rho_s = 0.5$ , regardless of the network topology. Note that the symmetry cannot be predicted by SCT in the sense that in case of completely independent self-loop weights  $n_D$  will monotonically decrease to  $1/N$  as  $\rho_s$  increases to 1, implying that a single driver node can fully control the whole network [20]. The symmetry can be theoretically predicted (see SM Sec.2.2). An immediate but counterintuitive result from the symmetry is that  $n_D$  in the absence of self-loops is exactly the same as

the case that each node has a self-loop with identical weight. This is a direct consequence of Kalman's rank condition for

controllability [1]:

$$\text{rank}[B, AB, \dots, A^{N-1}B] = \text{rank}[B, (A + w_s I_N)B, \dots, (A + w_s I_N)^{N-1}B] \quad (2)$$

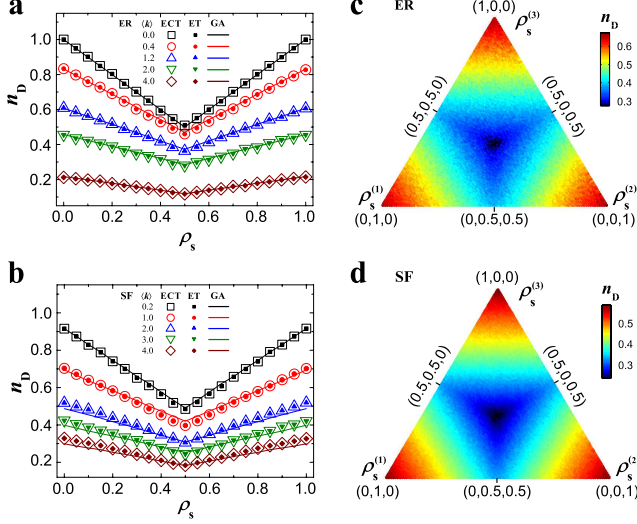


FIG. 2: (a)-(b) controllability measure  $n_D$  in the presence of a single type of nonzero self-loops with fraction  $\rho_s$  for random (ER) networks (a) and scale-free (SF) networks (b) with different average degree  $\langle k \rangle$ . (c)-(d)  $n_D$  of ER (c) and SF networks (d) with three types of self-loops  $s_1, s_2$  and  $s_3$  with density  $\rho_s^{(1)}, \rho_s^{(2)}$  and  $\rho_s^{(3)}$ , respectively. ECT denotes the results obtained from the exact controllability theory, ET denotes the results obtained from the efficient tool and GA denotes the results obtained from the graphical approach (see SM Sec.3). The color bar denotes the value of  $n_D$  and the coordinates in the triangle stands for  $\rho_s^{(1)}, \rho_s^{(2)}$  and  $\rho_s^{(3)}$ . The networks are described by structured matrix  $A$  and their sizes in (a)-(d) are 2000. The results from ECT and ET are averaged over 30 different realizations, and those from GA are over 200 realizations.

where the left and the right hand sides are the rank of controllability matrix in the absence and full of identical self-loops, respectively (see SM Sec.1 for proof).

The presence of two types of nonzero self-loops  $s_2$  and  $s_3$  leads to even richer behavior of controllability. If the three types of self-loops (including self-loops of zero weights) are randomly distributed at nodes, the impact of their fractions on  $n_D$  can be visualized by mapping the three fractions into a 2D triangle (or 2-simplex), as shown in Fig. 2c,d. We see that  $n_D$  exhibits symmetry in the triangle and the minimum  $n_D$  occurs at the center that represents identical fractions of the three different self-loop types. The symmetry-induced highest

controllability can be generalized to arbitrary number of self-loops. Assume there exist  $n$  types of self-loops  $s_1, \dots, s_n$  with weights  $w_s^{(1)}, \dots, w_s^{(n)}$ , respectively, we have

$$N_D = N - \min_i \left\{ \text{rank}(\Phi - w_s^{(i)} I_N) \right\} \quad (3)$$

for sparse networks with random weights (see SM Sec. 2 for detailed derivation and the formula of dense networks). An immediate prediction of Eq. (3) is that  $N_D$  is primarily determined by the self-loop with the highest density, simplifying Eq. (3) to be  $N_D = N - \text{rank}(\Phi - w_s^{\max} I_N)$ , where  $w_s^{\max}$  is the weight of the prevailing self-loop (see SM Sec. 2). Using Eq. (3) and the fact that  $\Phi$  is a mixed matrix, we can predict that  $N_D$  remains unchanged if we exchange the densities of any two types of self-loops (see SM Sec. 2), accounting for the symmetry of  $N_D$  for arbitrary types of self-loops. Due to the dominance of  $N_D$  by the self-loop with the highest density and the exchange-invariance of  $N_D$ , the highest controllability with the lowest value of  $N_D$  emerges when distinct self-loops are of the same density.

To validate the symmetry-induced highest controllability predicted by our theory, we quantify the density heterogeneity of self-loops as follows:

$$\Delta \equiv \sum_{i=1}^{N_s} \left| \rho_s^{(i)} - \frac{1}{N_s} \right|, \quad (4)$$

where  $N_s$  is the number of different types of self-loops (or the diversity of self-loops). Note that  $\Delta = 0$  if and only if all different types of self-loops have the same density, i.e.,  $\rho_s^{(1)} = \rho_s^{(2)} = \dots = \rho_s^{(N_s)} = \frac{1}{N_s}$ , and the larger value of  $\Delta$  corresponds to more diverse case. Figure 3a,b shows that  $n_D$  monotonically increases with  $\Delta$  and the highest controllability (lowest  $n_D$ ) arises at  $\Delta = 0$ , in exact agreement with our theoretical prediction. Figure 3c,d display  $n_D$  as a function of  $N_s$ . We see that  $n_D$  decreases as  $N_s$  increases, suggesting that the diversity of individual dynamics facilitates the control of a networked system. When  $N_s = N$  (i.e., all the self-loops are independent),  $n_D = 1/N$ , which is also consistent with the prediction of SCT [8, 20].

In some real networked systems, dynamic units are captured by high-order individual dynamics, prompting us to

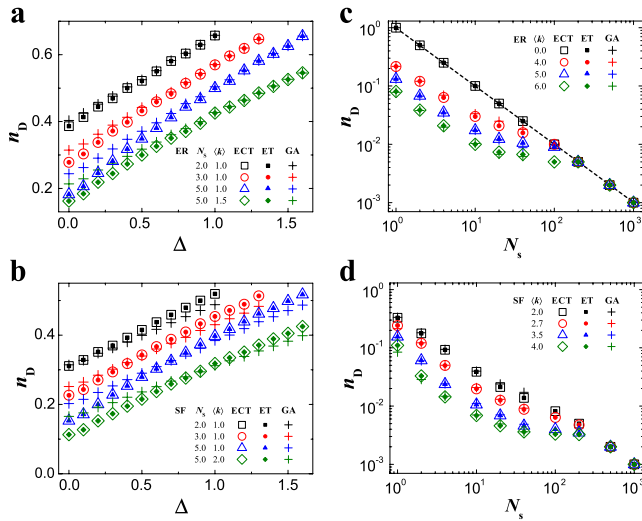


FIG. 3: **a-b**,  $n_D$  as a function of the density heterogeneity of self-loops ( $\Delta$ ) for ER (**a**) and SF (**b**) networks. **c-d**,  $n_D$  as a function of the number of different types of self-loops for ER (**c**) and SF (**d**) networks. The dotted line in (**c**) is  $n_D = 1/N_s$ . The networks are described by structured matrix  $A$  and their sizes in (**a**)-(**d**) are 1000. The results from ECT and ET are averaged over 30 different realizations, and those from GA are over 200 realizations. The notations are the same as Fig. 2.

check if the symmetry-induced highest controllability still holds for higher-order individual dynamics. The graph representation of dynamic units with 2nd-order dynamics is illustrated in Fig. 1b. In this case, the eigenvalues of the dynamic unit's state matrix  $\begin{pmatrix} 0 & 1 \\ a_0 & a_1 \end{pmatrix}$  play a dominant role in determining  $N_D$ . For two different units as distinguished by distinct  $(a_0 \ a_1)$  one can show that their state matrices almost always have different eigenvalues, except for some pathological cases of zero measure that occur when the parameters satisfy certain accidental constraints. The eigenvalues of the state matrix of dynamic units take over the roles of self-loops in the 1st-order dynamics, accounting for the following formulas for sparse networks

$$N_D = 2N - \min_i \left\{ \text{rank}(\Phi - \lambda^{(i)} I_{2N}) \right\}, \quad (5)$$

where  $\lambda^{(i)}$  is either one of the two eigenvalues of type- $i$  dynamic unit's state matrix. The formula implies that  $N_D$  is exclusively determined by the prevailing dynamic unit, (see SM Sec. 2). The symmetry of  $N_D$ , i.e., exchanging the densities of any types of dynamic units, does not alter  $N_D$  (see SM Sec. 2), and the emergence of highest controllability at the global symmetry point can be similarly proved as we did in the case of 1st-order individual dynamics.

The 3rd-order individual dynamics are graphically charac-

terized by a dynamic unit composed of three nodes (Fig. 1c), leading to a  $3N \times 3N$  state matrix (Fig. 1c). We can generalize Eq. (5) to arbitrary order of individual dynamics:

$$N_D = dN - \min_i \left\{ \text{rank}(\Phi - \lambda_d^{(i)} I_{dN}) \right\}, \quad (6)$$

where  $d$  is the order of the dynamic unit,  $\lambda_d^{(i)}$  is any one of the  $d$  eigenvalues of type- $i$  dynamic units and  $I_{dN}$  is the identity matrix of dimension  $dN$ . In analogy with the simplified formula for the 1st-order dynamics, insofar as a type of individual dynamics prevails in the system, Eq (6) is reduced to  $N_D = dN - \text{rank}(\Phi - \lambda_d^{\max} I_{dN})$ , where  $\lambda_d^{\max}$  is one of the eigenvalues of the prevailing dynamic unit's state matrix. Similar to the case of 1st-order individual dynamics, the global symmetry of controllability and the highest controllability occurs at the global symmetry point can be proved for individual dynamics of any order and arbitrary network topology (see SM Sec.2 and 3 for theoretical derivations and see SM Sec. 4 for numerical and analytical results of high-order individual dynamics).

In summary, we map individual dynamics into dynamic units that can be integrated into the matrix representation of the system, offering a general paradigm to explore the joint effect of individual dynamics and network topology on the system's controllability. The paradigm leads to a striking discovery: the universal symmetry of controllability as reflected by the invariance of controllability with respect to exchanging the fractions of any two different types of individual dynamics, and the emergence of highest controllability at the global symmetry point. These findings generally hold for arbitrary networks and individual dynamics of any order. The symmetry-induced highest controllability has immediate implications for devising and optimizing the control of complex systems by for example, perturbing individual dynamics to approach the symmetry point without the need to adjust network structure.

The theoretical paradigm and tools developed here also allow us to address a number of questions, answers to which could offer further insights into the control of complex networked systems. For example, we may consider the impact of general parameter dependency (e.g., link weight similarity), instead of focusing on self-loops or individual dynamics. Our preliminary results show that introducing more identical link weights will not affect the network controllability too much, unless the network is very dense and almost all link weights are identical (see SM Sec.5). We still lack a comprehensive understanding of the impact of parameter dependency on structural controllability for arbitrary complex networks. Moreover, at the present we are incapable of tackling general nonlinear dynamical systems in the framework of ECT, which is extremely challenging for both physicists and control theo-

rists. Nevertheless, we hope our approach could inspire further research interests towards achieving ultimate control of complex networked systems.

---

\* Electronic address: [yyl@channing.harvard.edu](mailto:yyl@channing.harvard.edu)

† Electronic address: [jjs@mit.edu](mailto:jjs@mit.edu)

- [1] R. E. Kalman, *J. Soc. Indus. and Appl. Math Ser. A* **1**, 152 (1963).
- [2] D. G. Luenberger, *Introduction to Dynamic Systems: Theory, Models, & Applications* (John Wiley & Sons, New York, 1979).
- [3] C. T. Lin, *IEEE Trans. Autom. Control* **19**, 201 (1974).
- [4] R. W. Shields, and J. B. Pearson, *IEEE Trans. Autom. Control* **21**, 203 (1976).
- [5] S. Hosoe, *IEEE Trans. Autom. Control* **25**, 1192 (1980).
- [6] C. Commault, J.-M. Dion, and J. W. van der Woude, *Kybernetika* **38**, 503 (2002).
- [7] J.-M. Dion, C. Commault, and J. van der Woude, *Automatica* **39**, 1125 (2003).
- [8] Y.-Y. Liu, J.-J. Slotine, and A.-L. Barabási, *Nature* **473**, 167 (2011).
- [9] T. Nepusz, and T. Vicsek, *Nature Phys.* **8**, 568-573 (2012).
- [10] Y.-Y. Liu, J.-J. Slotine, and A.-L. Barabási, *PLoS ONE* **7**, e44459 (2012).
- [11] W.-X. Wang, X. Ni, Y.-C. Lai, and C. Grebogi, *Phys. Rev. E* **85**, 026115 (2012).
- [12] Y. Tang, H. Gao, W. Zou, and J. Kurths, *PLoS ONE* **7**, e41375 (2012).
- [13] B. Wang, L. Gao, and Y. Gao, *J. Stat. Mech. : Theor. Exp.* **2012**, P04011 (2012).
- [14] M. Pósfai, Y.-Y. Liu, J.-J. Slotine, and A.-L. Barabási, *Sci. Rep.* **3**, 1067 (2013).
- [15] T. Jia, Y.-Y. Liu, E. Csóka, M. Pósfai, J.-J. Slotine, and A.-L. Barabási, *Nature Commun.* **4**, 2002 (2013).
- [16] G. Yan, J. Ren, Y.-C. Lai, C.-H. Lai, and B. Li, *Phys. Rev. Lett.* **108**, 218703 (2012).
- [17] R. Gutiérrez, I. Sendiña-Nadal, M. Zanin, D. Papo, and S. Boccaletti, *Sci. Rep.* **2**, 396 (2012).
- [18] Y.-Y. Liu, J.-J. Slotine, and A.-L. Barabási, *Proc. Natl Acad. Sci.* **110**, 2460-2465 (2013).
- [19] J. Sun, and A. E. Motter, *Phys. Rev. Lett.* **110**, 208701 (2013).
- [20] N. J. Cowan, E. J. Chastain, D. A. Vilhena, J. S. Freudenberg, and C. T. Bergstrom, *PLoS ONE* **7**, e38398 (2012).
- [21] Z. Yuan, C. Zhao, Z. Di, W.-X. Wang, and Y.-C. Lai, *Nature Commun.* **4**, 2447 (2013).
- [22] E. D. Sontag, *Mathematical Control Theory: Deterministic Finite Dimensional Systems* (Springer, 2nd edn, 1998).
- [23] P. J. Antsaklis, and A. N. Michel, *Linear Systems* (McGraw-Hill, 1997).
- [24] N. Cai, J.-X. Xi, Y.-S. Zhong, and H.-Y. Ma, *Int. J. Innov. Comput. I* **8**, 3315 (2012).
- [25] G. Parlangeli, and G. Notarstefano, *IEEE Trans. Autom. Control* **57**, 743 (2012).
- [26] G. Notarstefano, and G. Parlangeli, *IEEE Trans. Autom. Control* **58**, 1719 (2013).
- [27] J.-J. Slotine, and W. Li, *Applied Nonlinear Control* (Prentice-Hall, 1991).
- [28] K. Murota, *Matrices and Matroids for Systems Analysis* (Springer Heidelberg Dordrecht London, New York, USA, 2010).